Preliminary Safety Analysis of the Gorleben Site: Thermo-mechanical Analysis of the Integrity of the Geological Barrier in the Gorleben Salt Formation – 13307

R. Eickemeier*, S. Heusermann*, M. Knauth**, W. Minkley**, H.-K. Nipp* and T. Popp**
 Federal Institute for Geosciences and Natural Resources (BGR),
Stilleweg 2, D-30655 Hannover, Germany, heusermann@bgr.de
**Institute for Geomechanics (IfG),
Friederikenstraße 60, D-04279 Leipzig, Germany, wolfgang.minkley@ifg-leipzig.de

ABSTRACT

Exploration work at the Gorleben salt dome has been carried out since 1977 to investigate the site regarding its suitability as a final repository for high-level radioactive wastes. In the framework of the "Preliminary Safety Analysis of the Gorleben Site" a comprehensive assessment is being performed with focus on long-term safety. Because the integrity of the geological barrier is crucial for protection from damage caused by ionising radiation during the post-operational phase, 2D and 3D thermo-mechanical calculations for a reference section through the salt dome were carried out, all looking at two different waste emplacement concepts: emplacement in drifts and in boreholes. The calculated stresses are the basis for evaluating the barrier integrity on the basis of the dilatancy criterion and the fluid pressure criterion.

INTRODUCTION

Investigations about the suitability of the Gorleben salt dome as a potential site for a geologic repository for high radioactive heat-generating waste began on the surface in 1977. This work was joined by underground exploration of the site beginning in 1983. The investigations were suspended for ten years from 2000 to 2010 as part of a moratorium. Parallel with renewal of the investigation activities, the Federal Ministry of the Environment, Nature Conservation and Nuclear Safety (BMU) initiated the project "Preliminary Safety Analysis of the Gorleben Site (VSG)" to assess the safety of the Gorleben salt dome on the basis of current knowledge.

Following the German safety requirements, released in 2010 by BMU, a crucial part of the VSG project is to analyze the integrity of the geological barrier in order to determine whether stresses, which occur over time as a result of the forecast behaviour of the geologic repository system, could violate the integrity of the barrier over the specified verification period. In other words, it was necessary to investigate whether the properties of the geological barrier forming the effective isolation system are maintained over the verification period. The Federal Institute for Geosciences and Natural Resources (BGR), Hannover, and the Institute for Geomechanics (IFG), Leipzig, were jointly responsible for implementing the geomechanically-oriented part of the integrity analysis considering two concepts: the emplacement of Pollux casks in drifts and the emplacement of BSK3 fuel element canisters in boreholes.

CRITERIA TO ASSESS THE BARRIER INTEGRITY

To assess the barrier properties of rock salt layers under the influence of thermo-mechanical effects associated with the release of heat in the emplacement zone, computer simulations are carried out on the geomechanical processes which give rise to the creation of micro-fractures due to mechanical damage or fluid-pressure-driven opening up of grain boundaries. Understanding this process is important because the migration paths created in this way could ultimately cause liquids to penetrate the emplacement zone. This conceptual procedure means that the assessment of the hydraulic barrier properties is undertaken on the basis of mechanical parameters. This involves the use of the dilatancy criterion and the fluid pressure criterion as proof of safety requirements [1].

Dilatancy criterion (Eq. 1): No damage of the rock fabric must occur as a result of cracking and the interlinking of intercrystalline pore space in response to deviatoric stress. The damage process is associated with dilatancy, i.e. an increase in volume caused by the development of micro-cracks and crack accumulations. The stress state when dilatancy gives rise to damage is called the dilatancy limit. In the visco-elastic-plastic model concept of IfG the ratio between the slope of the volumetric strain $d\varepsilon_{Vol}$ and the principal strain $d\varepsilon_1$ has to be lower or equal to 0:

$$\frac{d\varepsilon_{Vol}}{d\varepsilon_1} \leq 0 \qquad \text{(Eq. 1)}$$

Fluid pressure criterion (Eq. 2): The minimum principal stress σ_{min} in the barrier, plus any tensile strength σ_z which may be present, must be larger than the hypothetical fluid pressure p_{Fl} which could be postulated to exist at the analysed depth [2]. Only if this criterion is satisfied, i.e. the safety factor S should be higher than 1 , no fluid-pressure driven penetration of fluids into the rock will take place under the given stress state:

$$S = \frac{\sigma_{\min} + \sigma_Z}{p_{Fl}} > 1 \qquad \text{(Eq. 2)}$$

As an alternative, BGR uses a simplified description of this criterion: that the minimum principal stress must not fall below the value of the hydrostatic fluid pressure p_{Fl} assumed at the analysed depth [3].

$$p_{FL} - \sigma_{\min} < 0 \qquad \text{(Eq. 3)}$$

The integrity of the salt barrier is only ensured if both criteria are satisfied in a sufficiently thick zone around the underground workings of the repository, so that linked flow paths from the water-bearing horizons in the overburden down to the emplacement zone and as well an escape of hazardous material from the repository itself (e.g. due to generation of a gas pressure) can be excluded from a geomechanical point of view.

GEOLOGICAL AND GEOMECHANICAL MODELING

The following data are required to thermo-mechanically model the geologic repository: geological structure of the salt dome, including the cover rock and surrounding rock, as the basis for determining the homogenous zones; technological emplacement concept with emplacement geometry; initial formation temperature; initial formation stress state; thermal and mechanical material properties of the modeled homogenous zones.

Geology

To describe the geological structure of the Gorleben salt dome, the geological cross-section through the EB1 investigation level along the 1W cross passage was used [4]. The following homogenous zones with exclusive elastic material properties were taken into consideration (Fig. 1): Quaternary (q), Tertiary (t), cap rock (cr), Upper Cretaceous (kro), Lower Cretaceous (kru), Jurassic – Keuper (j – k), Bunter Sandstone (so – su), Rotliegendes (r), Hauptanhydrit (z3HA).

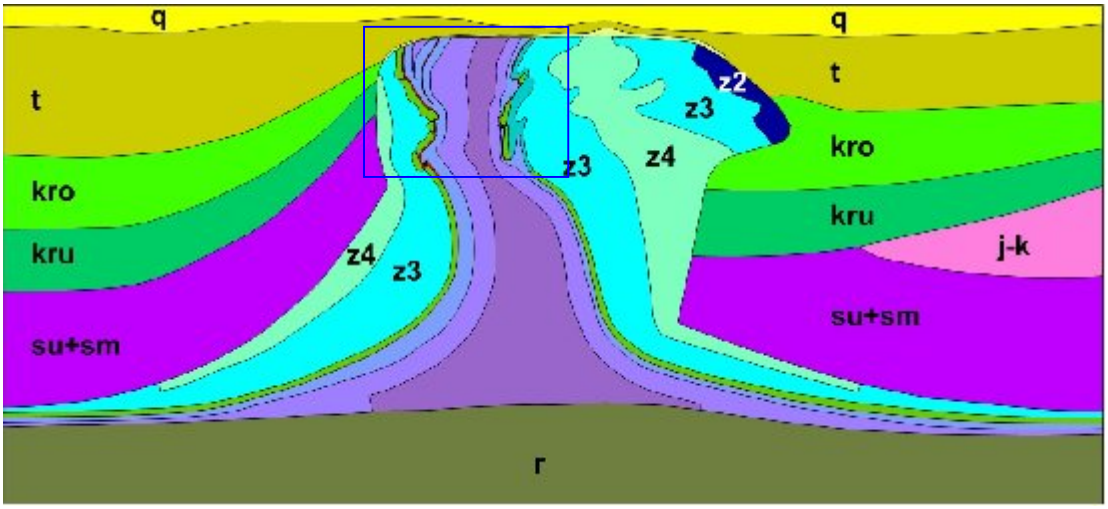

Fig. 1. Simplified geological model with homogenous zones (overview). The rectangle indicates the detailed section of Fig. 2.

In addition to the stiff Hauptanhydrit (z3HA) differentiation was also made between the following creepable homogenous zones in the vicinity of the EB1 investigation zone (Fig. 2): Liniensalz (z3LS), Kaliflöz Staßfurt (z2SF), Hauptsalz/Kristallbrockensalz (z2HS3), Hauptsalz/Streifensalz (z2HS2), Hauptsalz/Knäuelsalz (z2HS1).

The following stratigraphic horizons are incorporated in the model as homogenous zones with creepable material properties in the distal zone from the emplacement field beyond the Hauptanhydrit (z3HA) and/or the Liniensalz (z3LS): Aller Series rock salt (z4), Leine Series rock salt (z3), Staßfurt Series rock salt (z2).

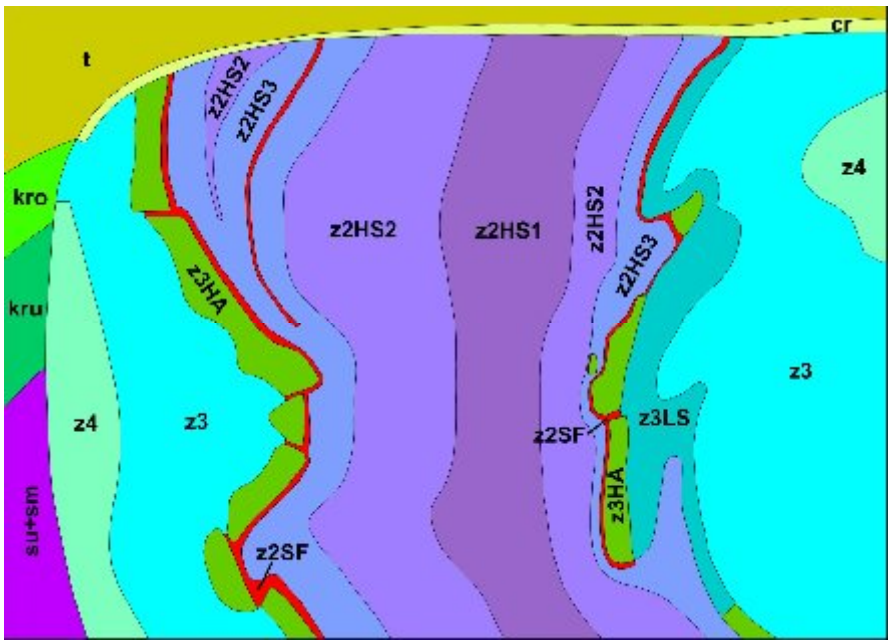

Fig. 2. Simplified geological model with homogenous zones (detailed diagram)

BGR-material models and parameters

The geomechanical behaviour of the creepable rock salt is modeled by using several material law variations which include elastic deformation and steady-state creep [5]. With respect to steady-state creep, the effective creep rate is determined as follows dependent on the temperature T and according to the BGR_a material law:

$$\dot{\varepsilon}_{eff}^{cr} = A \cdot e^{-\frac{Q}{R \cdot T}} \cdot \left(\frac{\sigma_{eff}}{\sigma^*} \right)^n \qquad \text{(Eq. 4)}$$

where R = universal gas constant ($8.3143 \cdot 10^{-3}$ kJ/mol/K), T = temperature (K), σ_{dev} = deviatoric stress (MPa), σ^* = reference stress (1.0 MPa), and the material parameters A = structural factor (0.18 1/d), n = stress exponent (5.0), and Q = activation energy (54.0 kJ/mol).

The BGR_b material law is used to determine the creep more precisely at higher temperatures taking into consideration two mutually independent deformation mechanisms:

$$\dot{\varepsilon}_{eff}^{cr} = \left[A_1 \cdot e^{-\frac{Q_1}{R \cdot T}} + A_2 \cdot e^{-\frac{Q_2}{R \cdot T}} \right] \cdot \left(\frac{\sigma_{eff}}{\sigma^*} \right)^n \qquad \text{(Eq. 5)}$$

where $A_1 = 2.3 \cdot 10^{-4}$ 1/d, $A_2 = 2.1 \cdot 10^{6}$ 1/d, $Q_1 = 42.0$ kJ/mol and $Q_2 = 113.4$ kJ/mol.

For carnallitite and brecciated carnallitite the specific material law BGR_{SF} is used (for details see [5]. The dilatant behaviour of rock salt has been considered using a dilatancy concept developed by BGR [6]. Here, the volumetric rate of dilatancy $\dot{\varepsilon}_{dil,vol}$ is correlated to the deviatoric creep rate, $\dot{\varepsilon}_{cr,dev}$ via an empirical relation using r_v (depending on σ_{dev} and the minimum compressive stress σ_{min}):

$$\dot{\varepsilon}_{dil,vol} = r_v \cdot \dot{\varepsilon}_{cr,dev} \qquad \text{(Eq. 6)}$$

If the deviatoric stress σ_{dev} exceeds a boundary stress $\sigma_{dev,dil}$, the factor r_v is positive and dilatancy will occur:

$$r_v = 0.8165 \cdot \left| \frac{\sigma_{dev} - \sigma_{dev,dil}}{|\sigma_{min} - 1/3 * \sigma_{dev}|} \right|^2 \quad if \ \sigma_{dev} > \sigma_{dev,dil} \qquad \text{(Eq. 7)}$$

$$\sigma_{dev,dil} = b \cdot (\sigma_{min} - 1/3 * \sigma_{dev})^c \qquad \text{(Eq. 8)}$$

with empirical parameters b = 3.2, and c = 0.78.

IfG-material models and parameters

The visco-elastic-plastic material law developed for rock salt by IfG is based on a concept which incorporates time-independent and time-dependent elements. The overall deformation is a combination of the following deformation elements: elastic isotropic deformation, sustained elastic deformation component (KELVIN element), (deviatoric) elastic and viscous deformation element (MAXWELL element), plastic deformation element (generalised MOHR-COULOMB model with deconsolidation and dilatancy) (Fig. 3).

Deformation below the dilatancy limit is derived from:

$$\varepsilon = \varepsilon^e + \varepsilon^{en} + \varepsilon^v \qquad \text{(Eq. 9)}$$

whilst the following equation applies to total deformation above the dilatancy limit:

$$\varepsilon = \varepsilon^e + \varepsilon^{en} + \varepsilon^v + \varepsilon^p \qquad \text{(Eq. 10)}$$

The elastic deformation element ε^e and the sustained elastic deformation element ε^{en} are reversible; the viscous element ε^v and the plastic element ε^p are irreversible. The pure elastic deformation element is time-independent, whilst the sustained elastic element and the viscous element are time-dependent. Plastic deformation is rate-dependent. The primary and secondary creep phases in

the material model are described by the rheological models after KELVIN and MAXWELL. Tertiary creep when the failure limit is exceeded can also be incorporated by coupling the BURGERS model – which arises from the series-connection of a KELVIN and a MAXWELL body – and the plastic deconsolidation model [7].

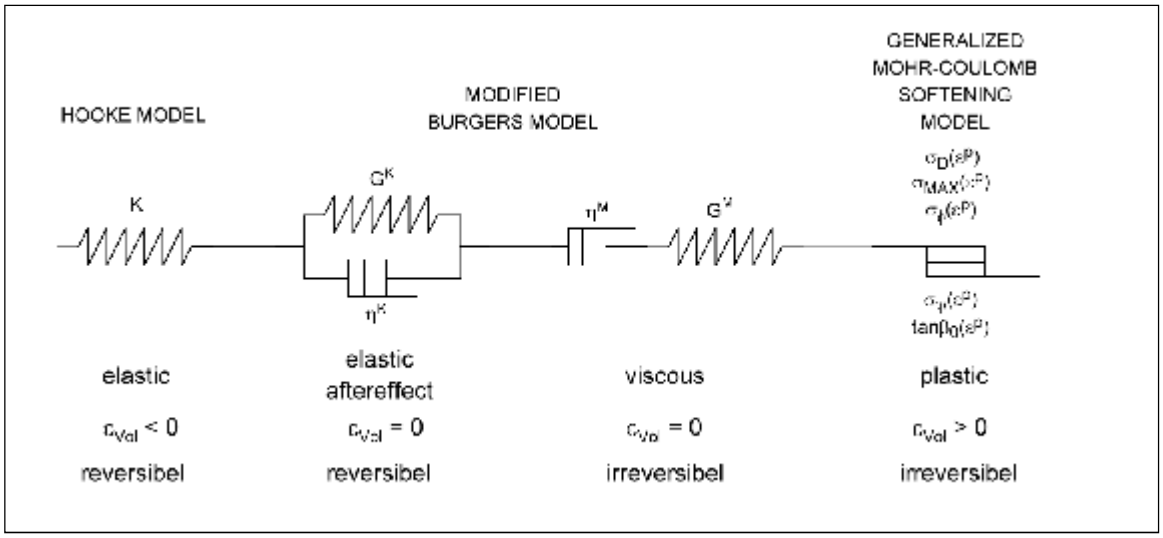

Fig. 3. Visco-elastic-plastic model concept from IfG

A flow and/or failure criterion for rock salt can be formulated in the form of a generalised non-linear MOHR-COULOMB flow criterion:

$$\sigma_{1B} = \sigma_D + N_\phi \cdot \sigma_3 \qquad \text{(Eq. 11)}$$

with the friction function:

$$N_\phi = 1 + \frac{\sigma_{MAX} - \sigma_D}{\sigma_\phi + \sigma_3} \quad \text{and} \qquad \text{(Eq. 12)}$$

$$\sigma_{eff,B} = \sigma_D + \frac{\sigma_{MAX} - \sigma_D}{\sigma_\phi + \sigma_3} \cdot \sigma_3 \qquad \text{(Eq. 13)}$$

where σ_3 is the minimum principal stress, σ_{1B} the maximum principal stress (failure stress), $\sigma_{eff,B} = \sigma_{1B} - \sigma_3$ the maximum effective stress, $\sigma_D(\varepsilon^P)$ the uniaxial compressive strength, $\sigma_{MAX}(\varepsilon^P)$ the maximum effective strength, $\sigma_\phi(\varepsilon^P)$ the curvature parameter of the strength curve, and ε^P the plastic shear deformation.

THERMO-MECHANICAL MODEL CALCULATIONS

2D models (IfG) and 3D models (BGR) were used for the thermo-mechanical calculations looking at the drift emplacement and the borehole emplacement concepts. The 2D models were used for detailed modeling of the proximal field in the emplacement zone, including the drifts and emplacement containers, as well as to investigate the thermal effects on the salt dome as a whole (far field). The 3D models were primarily used to model the spatial thermal effects in the far field, but did not take into consideration the underground workings in the mine. Because of the much coarser level of discretisation of the 3D model in the emplacement zone, instead of modeling the containers discretely, the generated heat was assumed to be homogenised over the emplacement zone.

An emplacement field with 10 emplacement drifts at the 870-m level was assumed in the calculations for the drift emplacement version. Drift emplacement is scheduled to use Pollux-10 casks which have a length of approx. 5.5 m, and a diameter of 1.56 m, and are emplaced within the drifts with spacings between the casks of 2.63 m. The drifts themselves are located 36 m apart.

The borehole emplacement version assumed that the BSK3 fuel element containers would be emplaced in 300 m deep boreholes with a separation between the boreholes of 50.6 m, and with seven emplacement boreholes per drift. The distance between the drifts from which the boreholes are drilled is 44 m in each case. The thermal output of the containers is calculated assuming they are filled with PWR-MIX 89/11 waste.

The calculations were carried out with different codes. While the IfG used the distinct-element code UDEC for its 2D calculations, BGR used the finite-element code JIFE for its 3D calculations. Different material laws are implemented in the two codes. In the IfG modeling, the verified lithological boundaries between the different Hauptsalz units are assumed to be potential bedding surfaces in the conservative approach taken, even though this is not supported by any location-specific findings.

Waste emplacement in drifts (2D modeling, IfG)

The numerical model is based on the homogenous zone model after Fig. 1. The model extends from the surface to a depth of 3,600 m and has a horizontal extent of over 5,300 m. It therefore encompasses a representative section of the salt dome for the integrity analysis. In addition to the emplacement drifts at the 870-m level, the modeling also incorporated the already existing investigation drifts at the 840-m level. All of the drifts were modeled as being excavated simultaneously in the first part of the simulation. The modeling then simulated the emplacement of the casks, and then the instant backfilling of the drifts with crushed salt.

The heat generated by each cask was simulated on the basis of the thermal output and decay times determined as part of the preceding thermal design calculations. Because the emplacement casks

in the 2D cross-section are represented by lateral quasi-infinitely extending casks, the thermal output during the course of the first decade from the start of emplacement was reduced to approx. 70 % to realistically incorporate the finite zone occupied by the casks and the lateral outflow of the heat into the space between the casks in the direction of the drifts.

The temperature at the surface of the casks rises very strongly at first to reach a first peak of around 185 °C only one year after emplacement within a central drift. The thermal conductivity of the crushed salt backfill rises with increasing compaction, which improves the dispersion of the heat and causes the temperature to drop as a consequence. The temperature rises again around six years after the start of emplacement because the temperature fields between neighbouring drifts now begin to overlap. This overlap in the central drifts causes the temperature to reach a second peak of approx. 190 °C, whilst the maximum in the outer drifts reaches a much lower temperature. The temperature in the emplacement zone decreases continuously after around 50 years as the heat spreads out into the far field. The maximum rise in temperature at top salt over the observed time period is approx. 6 °C.

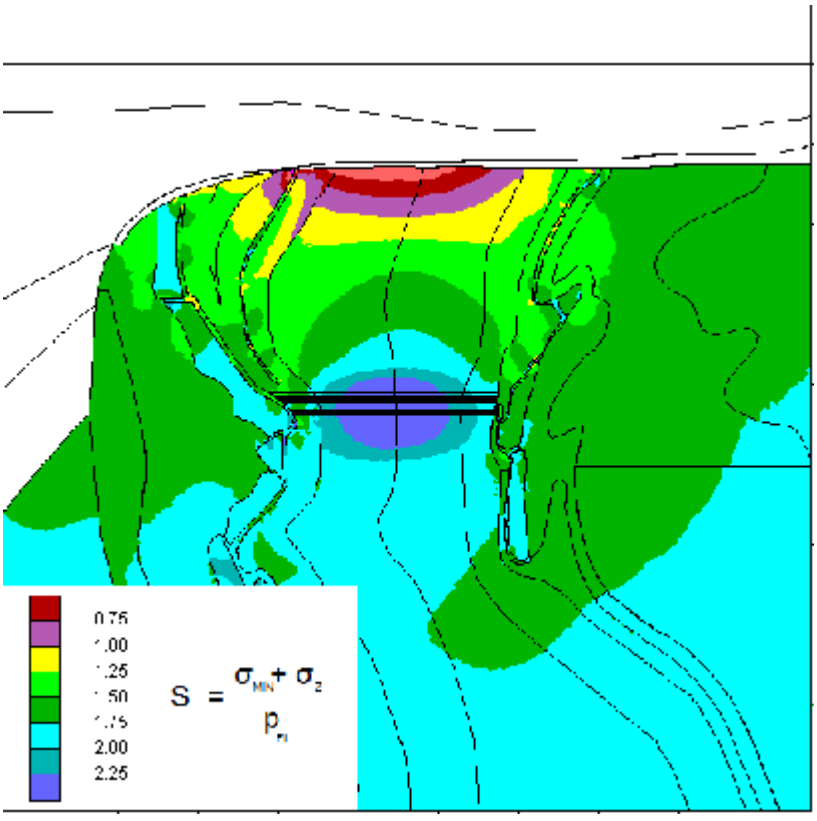

Fig. 4. Evaluation of the fluid pressure criterion 30 years after the start of emplacement. Criterion violation ($\eta_F < 1$) in the purple to red zone

Additional stresses are induced in the area surrounding the emplacement horizon by the heat generated by the radioactive waste and affecting the surrounding rock mass. On the one hand, the stresses give rise to dilatant damage to the rock fabric on the walls of the drifts, and on the other hand, cause the development of a zone with raised compressive stresses outside of the dilatant zone. This gives rise to uplift of the overlying rocks which extends up to the surface where the calculated uplift could reach up to 1.3 m. The thermo-mechanical calculations reveal that the stress state in the salt dome is modified over a large area as a result of the heating. A significant reduction in the minimum principal stress occurs at the top of the salt. The zone in which the fluid pressure criterion is temporarily violated has a maximum extent of down to approx. 150 m below top salt. The violations of the fluid pressure criterion extending to the greatest depth within the rock mass are calculated to be at the boundary horizon between the Streifensalz and Kristallbrockensalz, and the boundary horizon between the Kristallbrockensalz and the carnallitite (Fig. 4).

Dilatancy is almost exclusively restricted to the walls of the exploration and emplacement drifts, and only to a very minor extent away from the immediate surroundings of the drifts.

The calculations show that there is only local damage (mainly in the salt dome top region) and, therefore, no continuous violation of the integrity of top salt down to the emplacement horizon, i.e. no continuous pathway is created. The most serious consequences of the emplacement of heat-generating waste on the barrier integrity occur within the first 50 years after completing the emplacement procedure.

Waste emplacement in drifts (3D modeling, BGR)

The basis for generating the 3D model is the geological cross-section through the Gorleben salt dome shown in Fig. 1. The 3D model was generated by extruding a 2D model by exploiting a symmetry level – which meant that only half of the emplacement zone had to be modeled. As a conservative approach, underground workings are not taken into consideration in the 3D model.

The model zone encompasses a block with a width of 9 km and a depth of 4 km orthogonal to the strike of the salt structure. A horizontal extent of 5.4 km is incorporated in the direction of strike. The ten emplacement drifts in the model are 1.7 km long, and therefore represent an emplacement zone with a total length of 3.4 km on symmetry grounds. Temperature boundary conditions at the base of the model were defined as equivalent to the terrestrial heat flow acting in that position. A constant annual average of 8.5 °C was specified as the temperature boundary condition at the ground surface. In addition, a shearless, lithostatic-isotropic initial stress state was assumed. The calculations cover a period of 10,000 years after the start of emplacement.

The calculated temperature distribution is shown in Fig. 5 for the symmetry level of the model at time 82.1 years. This is the time when the maximum temperature of 169.9 °C is reached in the centre of the emplacement zone. The heat sources in the emplacement drifts are shown by

individual small concentric isotherms in the proximal zone of the drifts. At increasing distances from the emplacement drifts, the discrete heat sources act like a single homogenous heat source, and the isotherms are shown with ellipsoidal shapes in the zones of higher temperature rises.

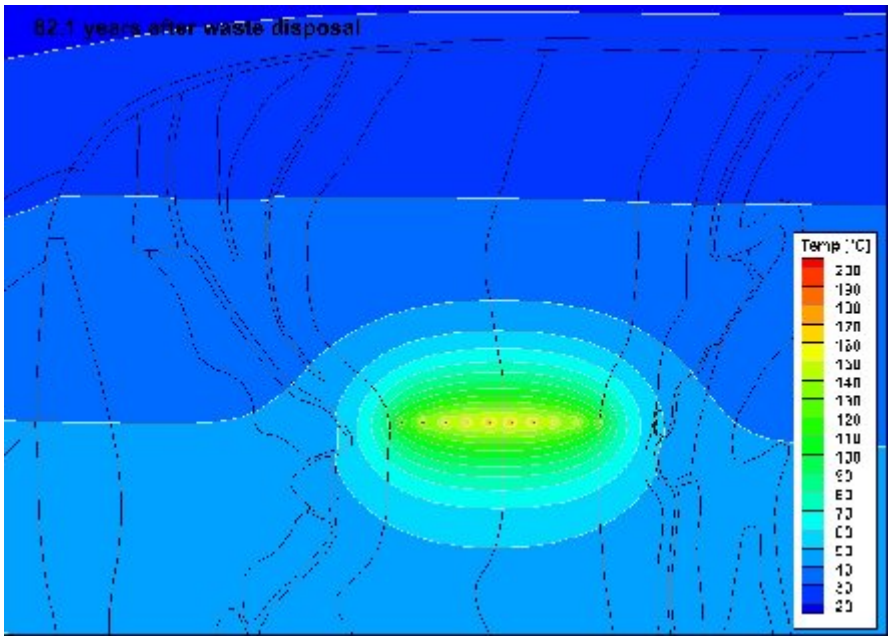

Fig. 5. Calculated temperatures at the symmetry level of the model for time 82.1 years

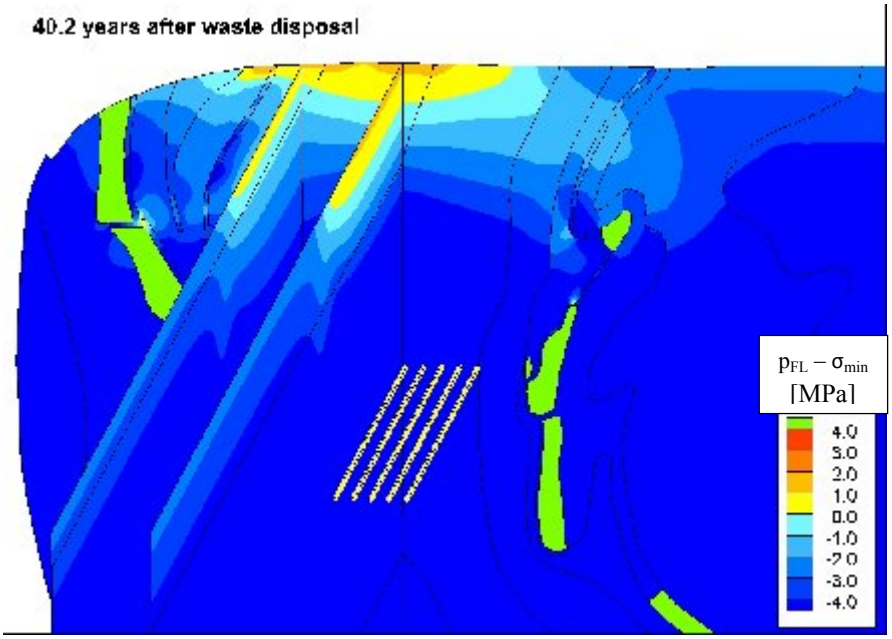

Fig. 6. 3D diagram showing the zones affected by fluid pressure at time 40.2 years

The calculated temperature distribution is shown in Fig. 5 for the symmetry level of the model at 82.1 years. This is the time when the maximum temperature of 169.9 °C is reached in the centre of the emplacement zone. The heat sources in the emplacement drifts are shown by individual small concentric isotherms in the proximal zone of the drifts. At increasing distances from the emplacement drifts, the discrete heat sources act like a single homogenous heat source, and the isotherms are shown with ellipsoidal shapes in the zones of higher temperature rises.

The fluid pressure criterion in the symmetry level within the Hauptsalz horizons (z2HS) is violated down to a maximum depth of 90 m below the top of the salt (Fig. 6). The spatial extent of the affected zones reduces over time and is no longer measurable after approx. 1,330 years. The spatial extent of the zones in which the fluid pressure criterion is violated remains restricted to the zones at the top of the salt lying directly above the emplacement zone. The maximum extent of the dilatant zones is reached after 10,000 years. It remains very tightly restricted to the zones in the Kristallbrockensalz lying directly above the emplacement zone. The dilatant zone does not impinge on rocks with potential migration paths, which means that no new paths for the infiltration of solutions are created.

Waste emplacement in boreholes (2D modeling, IfG)

The structure of the geological model is identical to the 2D study looking at drift emplacement. Only the position, the geometry and the number of emplacement drifts have been modeled differently in accordance with the borehole emplacement concept. In different modeling approaches, either a homogenised heat source covering a large area (see [3]) or an extracted temperature field based on a full 3D thermal simulation (performed by DBE) was used as a simplification for the 2D modeling of the planned hexagonal borehole arrangement. In the homogenised heat source approach, the thermal output of an individual container is converted into a specific homogenised output taking into consideration the length of the borehole and the catchment area of a borehole in a system with a hexagonal layout. This output is then applied homogenously within the emplacement zone. In the case of the borehole emplacement version as well, the thermal energy which flows out of the radioactive waste into the rock mass induces additional stresses in the vicinity of the emplacement horizon because of the suppression of heat dispersion. Compared to drift emplacement, the larger overall output in the model cross-section gives rise to slightly higher uplift calculated in the overlying rock formations. This uplift has still not reached its peak after 1,000 years from the beginning of emplacement, and has already reached up to 3.5 m on the ground surface by this time. In this emplacement version as well, there is a calculated reduction in the minimum principal stress at the top salt zone. The maximum zone in which the fluid pressure criterion is violated extends down to around 210 m below top salt. Compared to the drift emplacement, the larger heat output overall in this model cross-section therefore also gives rise to a violation of the fluid pressure criterion (Fig. 7) which extends deeper into the rock mass.

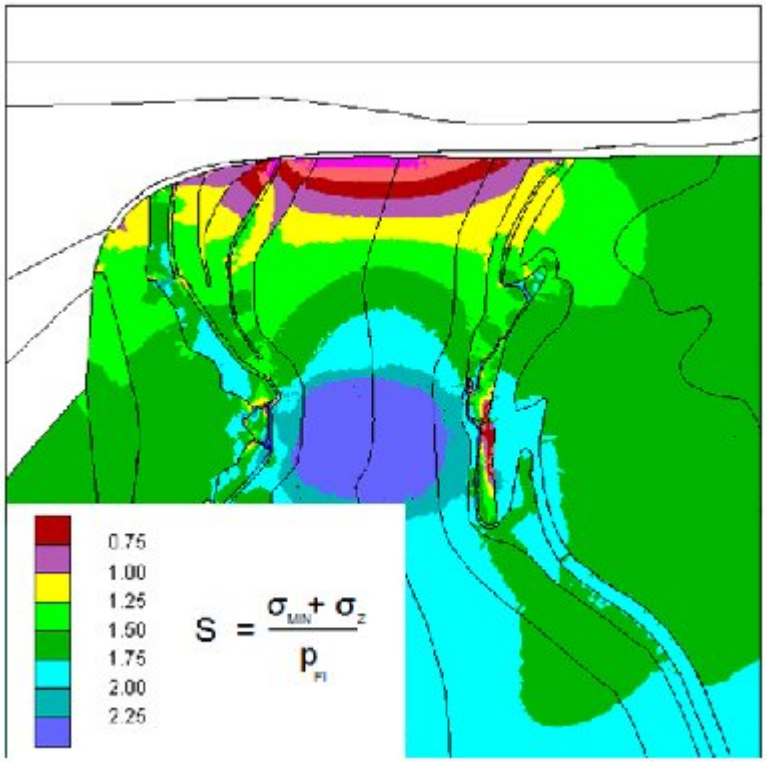

Fig. 7. Evaluation of the fluid pressure criterion after time equals 30 years from the beginning of emplacement

Waste emplacement in boreholes (3D modeling, BGR)

The 3D model for the borehole emplacement concept was generated on the basis of the geological cross-section shown in Fig. 1. The 3D model was generated by extruding a 2D model by exploiting a symmetry level – which meant that only half of the emplacement zone had to be modeled.

The model zone encompasses a block with a width of 9 km and a depth of 4 km orthogonal to the strike of the salt structure. A horizontal extent of 6.0 km is incorporated in the direction of strike. The drifts required to drill the emplacement boreholes run orthogonal to the strike of the salt dome and have a mutual separation of 44.0 m, and the boreholes in the drifts are separated by a distance of 56.0 m. An emplacement zone with a half length of 575 m is modeled in the strike direction of the salt dome so that the total length of the simulated emplacement zone is 1.15 km. Seven emplacement boreholes with a separation of 56.0 m were taken in consideration in each case. The temperature distribution after 345 years at the symmetry level is shown in Fig. 8. At this point in time, the maximum temperature of 198.4 °C is reached in the centre of the emplacement zone.

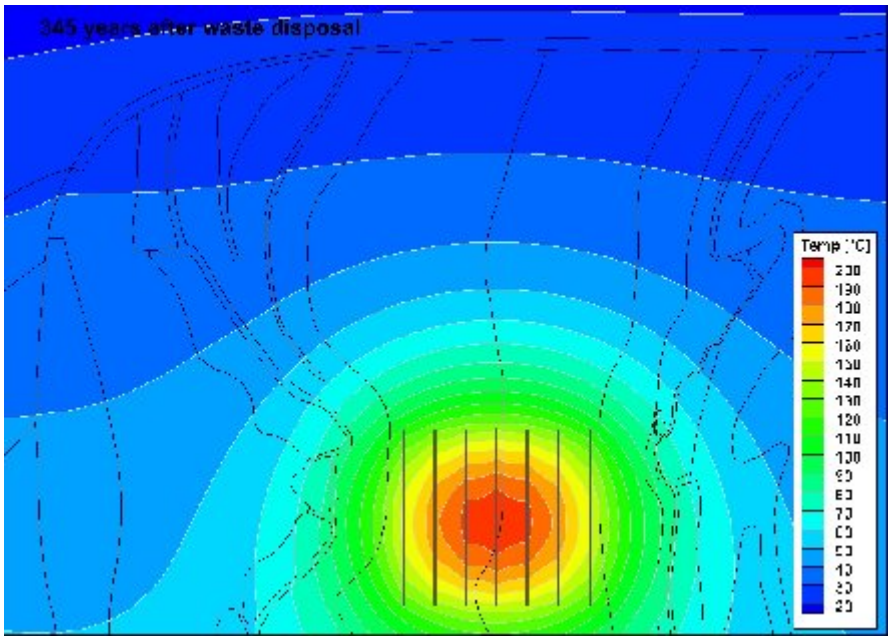

Fig. 8. Calculated temperature distribution at the symmetry level of the model after 345 years

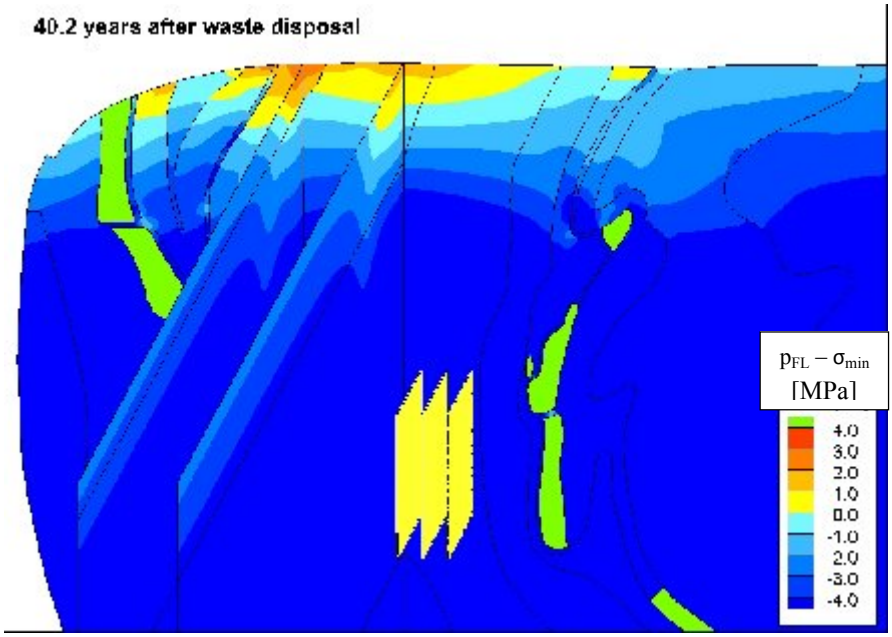

Fig. 9. Evaluation of the fluid pressure criterion after time equals 40.2 years

The fluid pressure criterion in the symmetry level within the Hauptsalz horizons (z2HS) is violated down to a maximum depth of 120 m below top salt (Fig. 9). The spatial extent of the affected zones reduces over time and is no longer measurable after approx. 3,270 years. The spatial extent of the zones in which the fluid pressure criterion is violated remains tightly restricted to zones at the top of the salt lying directly above the emplacement zone. In the direction of strike as well, the dilatant zone exclusively extends in the zone bounded by the length of the emplacement zone. The dilatant zone does not impinge on rocks with potential migration paths, which means that no new paths for the infiltration of solutions are created by this effect.

CONCLUSIONS

The emplacement of heat-generating high radioactive waste gives rise to temperature changes in the rock mass which itself causes stress and deformation changes, and can diminish the integrity of the geological barrier. Thermo-mechanical simulations carried out by BGR and IfG with a range of codes and material laws produced the following results:

- Although the emplacement of heat-generating waste can cause the salt dome to heat up over a large area, the thermally-induced stresses do not give rise to any continuous migration paths.
- The highest thermo-mechanical stresses affecting the salt barrier occur within the first hundred years after sealing the geologic repository, so that the loss of integrity of the barrier becomes increasingly unlikely in the time periods that follow.
- Mechanical damage caused by exceeding the dilatancy limit affects mainly the area adjacent to the underground cavities, but otherwise are very localised in the top salt zone and are only of secondary importance with respect to the integrity of the salt barrier.
- The possibilities of fluids from the cap rock penetrating the salt structure is a crucial aspect. The calculations confirmed that temporary local violations of integrity initiated at the top of the salt could penetrate down to approx. 130 m into the salt dome. However, they terminate several hundred metres above the emplacement horizons and therefore still leave in place a thick intact barrier. If in the hypothetical extreme case, the steeply dipping stratigraphic boundary horizons reaching up at the top of the salt are assumed to be potential zones of weakness with reduced shear strength, the temporary violation of integrity could extend as far as a few hundred metres into the salt dome. However this would still leave an adequately thick intact barrier in place.
- The thermo-mechanical stresses calculated for the borehole emplacement concept are higher than those calculated for the drift emplacement concept because the heat is released in a more concentrated area.
- Future safety analyses should also involve more detailed investigations (e.g. with respect to experimental investigations of the stratigraphic boundary horizons, mechanical description of

the shear behaviour, the pressure-driven infiltration of fluids along stratigraphic boundary horizons within salt rock masses, coupled THM calculations on fluid infiltration into the barriers).

REFERENCES

1. BMU: Sicherheitsanforderungen an die Endlagerung wärmeentwickelnder radioaktiver Abfälle (Stand: 30.09.2010). Bundesministerium für Umwelt, Naturschutz und Reaktorsicherheit (BMU), Bonn, Germany (2010).
2. Minkley, W. and Popp, T.: Final Disposal in Rock Salt – Geomechanical Assessment of the Barrier Integrity. *Proc. 44th US Rock Mechanics Symposium*, ARMA, Salt Lake City (2010).
3. Nipp, H.-K. and Heusermann, S.: Erkundungsbergwerk Gorleben – Gebirgsmechanische Beurteilung der Integrität der Salzbarriere im Erkundungsbereich EB1 für das technische Endlagerkonzept 1 (Bohrlochlagerung, BSK3). Bericht, Bundesanstalt für Geowissenschaften und Rohstoffe (BGR), Hannover, Germany (2000).
4. Bornemann, O., Behlau, J., Fischbeck, R., Hammer, J., Jaritz, W., Keller, S., Mingerzahn, G. and Schramm, M.: *Description of the Gorleben Site - Part 3: Results of the geological surface and underground exploration of the salt formation*. Federal Institute for Geosciences and Natural Resources (BGR), 223 p., Hannover, Germany (2008).
5. Bräuer, V., Eickemeier, R., Eisenburger, D., Grissemann, C., Hesser, J., Heusermann, S., Kaiser, D., Nipp, H.-K., Nowak, T., Plischke, I., Schnier, H., Schulze, O., Sönnke, J. and Weber, J.R.: *Description of the Gorleben Site - Part 4: Geotechnical exploration*. Federal Institute for Geosciences and Natural Resources (BGR), 176 p., Hannover, Germany (2011).
6. Hunsche, U. and Schulze, O.: The dilatancy concept - a basis for the modelling of coupled TMH processes in rock salt. *European Commission CLUSTER Conference on the Impact of EDZ on the Performance of Radioactive Waste Geological Repositories*, Nov. 3-5, 2003, Luxembourg (2003).
7. Minkley, W. and Mühlbauer, J.: Constitutive models to describe the mechanical behavior of salt rocks and the imbedded weakness planes. *The Mechanical Behavior of Salt – Understanding of THMC Processes in Salt*, (Eds. M. Wallner, K.-H. Lux, W. Minkley & H.R. Hardy, Jr.), p. 119-127, Taylor and Francis Group, London (2007).

ACKNOWLEDGMENTS

This research was partially funded by the Federal Ministry of the Environment, Nature Conservation and Nuclear Safety of Germany.